Parameter identification of computational fracture models

C. Iacono & L. J. Sluys
Faculty of Civil Engineering and Geosciences, Delft University of Technology.
Delft, The Netherlands.

J. G. M. van Mier
ETH Hönggerberg, Institute for Building Materials, Zürich, Switzerland.

ABSTRACT: Fracture mechanics problems for quasi-brittle materials may be analyzed using non-local or gradient enhanced damage models. These models are able to reproduce localization phenomena and size effects by the introduction of an internal length scale parameter. However, the correct determination of the model parameters heavily determines the reliability of the model. Direct identification of the internal length scale and the constitutive softening law parameters is not possible and an inverse procedure is required. This paper presents some issues related to the identification (inverse) problem of the gradient enhanced continuum damage model. The experimental data of tensile size effect tests on dog-bone shaped specimens are used with two different parameter identification techniques: the Kalman filter method and the K-Nearest Neighbors method.

1 INTRODUCTION

Inverse problems stand in contrast to direct problems. In the direct problem the objective is the analytical or numerical solution of ordinary or partial differential equations, knowing initial conditions, boundary conditions and equation constants (model parameters). The unknown quantities are dependent variables (as stress, strain or displacement) that depend also on the model parameters. Experimental measurements are not involved in the solution of direct problems. In contrast, the model parameters represent the main objective of the inverse problem. A spatially and/or temporally distributed amount of measurements is required for this purpose. The comparison of the measurements with the corresponding computational values is necessary for the parameter identification. The solution of the inverse problem is represented by the parameter set that corresponds to the best match between computational and corresponding experimental values. The parameter identification problem requires appropriate experiments and an appropriate inverse technique (Beck & Arnold 1977).

This paper presents the parameters estimation problem related to the elasticity based gradient-enhanced continuum damage model used to describe fracture phenomena in quasi-brittle materials such as concrete and rock. In particular, the determination of the internal length parameter and the softening law parameters are of prime interest.

A brief presentation of the model is given in Section 2. In Section 3 the inverse problem is formulated and the Kalman Filter (KF) method and the K-Nearest Neighbors (KNN) method are briefly described. In Section 4 the numerical results of the two inverse techniques applied to the experimental data of tensile size effect tests are presented.

2 NUMERICAL MODEL

2.1 *Local damage model*

The isotropic, quasi-brittle elasticity based damage model (Lemaitre & Chaboche 1990) is given by

$$\boldsymbol{\sigma} = \left(1-\omega\right)\mathbf{D}^{el}\boldsymbol{\varepsilon} \tag{1}$$

in which $\mathbf{D}^{el}$ is the matrix of the virgin elastic stiffness moduli and the scalar variable ω represents the damage which grows from zero (elastic material) to one (completely damaged material).

If an invariant measure of strain, the equivalent strain ε_{eq}, is defined, the damage process starts

when $\varepsilon_{eq} = \kappa_i$, being κ_i a strain threshold for damage evolution.

A history variable κ can be defined, representing the most severe deformation undergone by the material:

$$\kappa(\varepsilon_{eq}) = \max(\varepsilon_{eq}, \kappa_{\max}) \tag{2}$$

where κ_{max} is the maximum value of equivalent strain occurred in the material.

The damage variable ω is a function of the history variable κ according to a damage evolution law that governs the growth of damage:

$$\omega = \omega(\kappa) \tag{3}$$

Whether damage growth is possible is determined on the basis of a loading function expressed in terms of the equivalent strain:

$$f(\varepsilon_{eq}) = \varepsilon_{eq} - \kappa(\varepsilon_{eq}) \tag{4}$$

with the following Kuhn-Tucker relations

$$f\dot{\kappa} = 0 \quad f \le 0 \quad \dot{\kappa} \ge 0 \tag{5}$$

For the equivalent strain, the modified von Mises definition (Vree et al. 1995) is adopted:

$$\varepsilon_{eq} = \frac{(\eta-1)I'_1}{2\eta(1-2\nu)} + \frac{1}{2\eta}\sqrt{\frac{(\eta-1)^2 I'^2_1}{(1-2\nu)^2} + \frac{12\eta J'_2}{(1+\nu)^2}} \tag{6}$$

where I'_1 and J'_2 are the first invariant of the strain tensor and the second invariant of the deviatoric strain tensor, respectively, and η is a model parameter given by the ratio of the compressive and the tensile strength of the material: $\eta = f_{cc}/f_{ct}$.

The following exponential softening damage evolution law has been chosen

$$\omega = 1 - \frac{\kappa_i}{\kappa}[1 - \alpha + \alpha e^{-\beta(\kappa-\kappa_i)}] \tag{7}$$

where α and β are two additional model parameters that govern the softening curve. As schematically represented in Figure 1, α determines the residual stress of the damaged material, and β the (negative) slope of the softening branch.

The standard local damage model presents what is commonly known as *mesh dependence*: the width of the process zone depends on the finite element size. This result is mathematically explained by a local loss of ellipticity of the set of partial differential equations that governs the rate of deformation. Mechanically the phenomenon can be seen as the lack of a localization limiter, related to the micro-structure of the material, that can be introduced adopting a nonlocal approach.

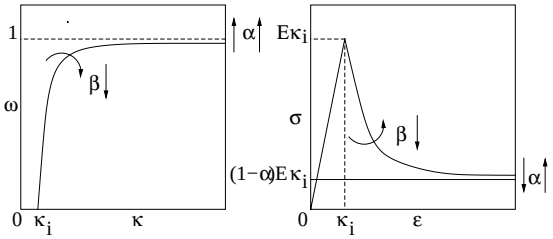

Figure 1. Exponential softening damage evolution law and uniaxial stress-strain curve.

2.2 *Nonlocal model: gradient-enhanced formulation*

In a nonlocal generalization (Bažant & Pijaudier-Cabot 1987, 1988) a nonlocal equivalent strain $\bar{\varepsilon}_{eq}$ is introduced, defined as the following spatially averaged quantity:

$$\bar{\varepsilon}_{eq}(\boldsymbol{x}) = \frac{1}{\int_\Omega \Psi(\boldsymbol{y};\boldsymbol{x})d\Omega} \int_\Omega \Psi(\boldsymbol{y};\boldsymbol{x})\bar{\varepsilon}_{eq}(\boldsymbol{y})d\Omega \tag{8}$$

where **y** points to the positions of the infinitesimal volume dΩ. The length scale parameter is related to the size of neighborhood considered for the spatial average of Equation 8. The homogeneous and isotropic Gauss distribution is usually adopted for the weight function $\Psi(\boldsymbol{y};\boldsymbol{x})$.

The constitutive equations are similar to those presented in Section 2 replacing the local equivalent strain $\varepsilon_{eq}(\boldsymbol{x})$ by the nonlocal counterpart $\bar{\varepsilon}_{eq}(\boldsymbol{x})$.

In a gradient damage formulation the integral Equation 8 can be approximated by the following partial differential equation (Peerlings et al. 1996)

$$\bar{\varepsilon}_{eq} - c\nabla^2\bar{\varepsilon}_{eq} = \varepsilon_{eq} \tag{9}$$

where $\nabla^2 = \sum_i \partial^2/\partial x_i^2$ and c is the gradient parameter related to the internal length scale.

The numerical implementation of the gradient-enhanced damage model in the finite element framework requires the spatial discretisation, by means of different shape functions, of the displacement field $\boldsymbol{u}$ and of the nonlocal equivalent strain $\bar{\varepsilon}_{eq}$ (Peerlings 1999).

The n_x model parameters can be assembled in the following vector

$$\mathbf{x} = [\mathrm{E} \quad \nu \quad \kappa_i \quad \alpha \quad \beta \quad c \quad \eta]^T \tag{10}$$

where

E = Young's modulus
ν = Poisson's ratio
κ_i = strain threshold for damage initiation
α = softening curve parameter
(related to the residual stress)
β = softening curve parameter
(related to the slope of the softening branch)
c = gradient parameter
η = ratio of compressive and tensile strength f_{cc}/f_{ct}

The inverse problem consists therefore in identifying the **x** vector.

3 INVERSE PROBLEM

The main elements involved in the formulation of an inverse problem are the numerical (forward) model, the experiment and the inverse technique. During laboratory tests, n_y observable quantities (e.g. forces, displacements etc.) can be measured at different "instants" t and collected in a vector $\mathbf{y}^t_{exp}$ for t=1,2,3....n_t.

The corresponding quantities may be computed by the numerical model and collected in the vector $\mathbf{y}^t_{comp}(\mathbf{x})$, depending on the model parameters vector **x** given by Equation 10.

The inverse technique deals with both vectors $\mathbf{y}^t_{exp}$ and $\mathbf{y}^t_{comp}(\mathbf{x})$, and sets the comparison criterion between them. The parameter estimation is the parameter set corresponding to $\mathbf{y}^t_{comp}$ that matches the best with the comparison criterion.

3.1 *K-Nearest Neighbors Method (KNN)*

The criterion adopted by this method is related to the distance between the two vectors $\mathbf{y}^t_{exp}$ and $\mathbf{y}^t_{comp}$.

Once a population of parameters sets $\mathbf{x}_i$ is chosen, with i=1,2,3....n_p, the corresponding vectors $\mathbf{y}_{comp}(\mathbf{x}_i)$ can be computed by the numerical model as a solution of the forward problem presented in Section 2. All the measurements are considered in a batch form so that the superscript index t disappears (i.e. t=1). Hence for each $\mathbf{y}_{comp}$ the corresponding Euclidean distance from $\mathbf{y}_{exp}$ may be easily evaluated. The solution of the parameter identification problem is the parameter set **x** that corresponds to the minimum distance between $\mathbf{y}_{exp}$ and $\mathbf{y}_{comp}$. In other words, the identified parameters set is the vector **x** that corresponds to the nearest neighbor, denoted as K=1, $\mathbf{y}_{comp}$ of $\mathbf{y}_{exp}$.

Since the experimental vector $\mathbf{y}_{exp}$ is affected by errors and uncertainties, an obvious refinement of the method is to weight the contribution of the various measurements with the associated error covariance. Hence for each parameter set $\mathbf{x}_i$ the following function (weighted squared distance) has to be evaluated:

$$f(\mathbf{x}) = (\mathbf{y}_{comp}(\mathbf{x}) - \mathbf{y}_{exp})^T \mathbf{C}_{exp}^{-1} (\mathbf{y}_{comp}(\mathbf{x}) - \mathbf{y}_{exp})^T = \mathbf{e}(\mathbf{x})^T \mathbf{C}_{exp}^{-1} \mathbf{e}(\mathbf{x}) \quad (11)$$

where the error $\mathbf{e}(\mathbf{x})$ is defined as the difference between the experimental and computational response and $\mathbf{C}_{exp}$ is the matrix of the error covariance of the measurements. If the measurements are independent and the errors have a zero mean, the weighting matrix $\mathbf{C}_{exp}$ reduces to a diagonal matrix, with the error variances s^2 as the diagonal components. The standard deviation s of repeated experiments under the same condition may be used to compute the $\mathbf{C}_{exp}$ matrix and Equation 11 becomes:

$$f(\mathbf{x}) = \sum_{j=1}^{n_y} \frac{1}{s_j^2} (y_{comp,j}(\mathbf{x}) - y_{exp,j})^2 \quad (12)$$

The solution of the parameter identification problem is given by

$$\hat{\mathbf{x}} = \min_{\mathbf{x}} \{ f(\mathbf{x}) \} \quad (13)$$

The KNN method is a derivative free procedure (i.e. no derivative of the objective function $f(\mathbf{x})$ has to be computed) and offers the advantage of parallel runs of different forward problems for the evaluation of $f(\mathbf{x})$ for each parameter set $\mathbf{x}_i$.

3.2 *Kalman Filter Method (KF)*

The basic notions of the mathematical formulation of the Kalman filter procedure are presented in Bolzon et al. (2002) (see also Iacono et al. 2003), and for detailed treatments see e.g. Kailath et al. (2000), Tarantola (1987), Bittanti et al. (1984), Catlin (1989), Bui (1994).

The solution of the forward problem depends on the model parameter vector **x** according to the following general relation:

$$\mathbf{y}^t_{comp} = \mathbf{h}_t(\mathbf{x}) \quad (14)$$

where $\mathbf{h}_t(\mathbf{x})$ is the *forward operator*. Here, the gradient-enhanced damage model is a nonlinear forward operator.

The Kalman filter technique solves the parameter identification problem in a statistical context. The following assumptions are considered herein:

- all the random variable vectors involved follow a Gaussian distribution
- the mathematical model, i.e. the forward operator $\mathbf{h}_t(\mathbf{x})$, is considered as deterministic
- measurements uncertainties, represented by the vector $\mathbf{v}_t$, are considered as Gaussian white noises (i.e. zero mean and $\mathbf{C}_{exp}$ covariance matrix).

Since the forward operator has been assumed as deterministic, the measurement noise $\mathbf{v}_t$ determines the difference between the experimental and computed observable quantities, which changes Equation 14 into

$$\mathbf{y}^t_{exp} = \mathbf{y}^t_{comp} + \mathbf{v}_t = \mathbf{h}_t(\mathbf{x}) + \mathbf{v}_t \tag{15}$$

Besides the experimental and computed data, the KF procedure relies also on an initial "a priori" estimate of the model parameter vector $\mathbf{x}$, that is assumed to be statistically defined by a Gaussian distribution with mean $\mathbf{x}_0$ and covariance matrix $\mathbf{C}_0$.

Starting from the two Gaussian distributions of the measurements uncertainty vector $\mathbf{v}_t$ and of the initial guess of the model parameters and manipulating the equations, the following optimization problem is obtained

$$\hat{\mathbf{x}} = \max_{\mathbf{x}} \left\{ f_{\mathbf{x}|\mathbf{y}}(\mathbf{x}, \mathbf{y}^t_{comp}) \right\} = \min_{\mathbf{x}} \left\{ S_t(\mathbf{x}) \right\} \tag{16}$$

where

$$f_{\mathbf{x}|\mathbf{y}}(\mathbf{x}, \mathbf{y}^t_{exp}) = \frac{1}{\mu} \exp\{-S_t(\mathbf{x})\} \tag{17}$$

$$S_t(\mathbf{x}) = (\mathbf{y}^t_{exp} - \mathbf{h}_t(\mathbf{x}))^T (\mathbf{C}^t_{exp})^{-1} (\mathbf{y}^t_{exp} - \mathbf{h}_t(\mathbf{x})) + (\mathbf{x} - \mathbf{x}_0)^T \mathbf{C}_0^{-1} (\mathbf{x} - \mathbf{x}_0) \tag{18}$$

and $\mu \equiv f_{\mathbf{y}}(\mathbf{y}_{exp})$ does not depend on the model parameter vector $\mathbf{x}$, and can be seen as a normalizing factor.

The parameter vector estimation $\mathbf{x}$ corresponds to the maximum conditional probability density given by Equation 17. If the forward operator $\mathbf{h}_t(\mathbf{x})$ is linear, then $f_{\mathbf{x}|\mathbf{y}}(\mathbf{x},\mathbf{y}^t_{exp})$ is a Gaussian (normal) distribution. However, this is not the case for the gradient-enhanced damage model considered here. In this case an iterative inverse procedure can still be formulated introducing a step-by-step linearization (1st-order Taylor expansion) of the forward operator and assuming a normal distribution of $f_{\mathbf{x}|\mathbf{y}}(\mathbf{x},\mathbf{y}^t_{exp})$ within each step. In this case the following set of equations can be obtained:

$$\mathbf{L}_t = \frac{\partial \mathbf{h}_t}{\partial \mathbf{x}}(\hat{\mathbf{x}}_{t-1}, t) \tag{19}$$

$$\mathbf{K}_t = \hat{\mathbf{C}}_{t-1}\mathbf{L}_t^T [\mathbf{L}_t \hat{\mathbf{C}}_{t-1} \mathbf{L}_t^T + \mathbf{C}^t_{exp}]^{-1} \tag{20}$$

$$\hat{\mathbf{x}}_t = \hat{\mathbf{x}}_{t-1} + \mathbf{K}_t (\mathbf{y}^t_{exp} - \mathbf{h}_t(\hat{\mathbf{x}}_{t-1})) \tag{21}$$

$$\hat{\mathbf{C}}_t = \hat{\mathbf{C}}_{t-1} - \mathbf{K}_t \mathbf{L}_t \hat{\mathbf{C}}_{t-1} \tag{22}$$

where the tangent operator $\mathbf{L}_t$ is denoted as *sensitivity matrix* and $\mathbf{K}_t$ as *gain matrix*.

Equations 19-22 define a recursive procedure that, filtering along the sequence of experimental data, gives at each step t a better estimate of the mean value of the model parameters and the corresponding covariance matrix. The initialization of the iterative scheme (i.e. for t=1) requires the initial guess $\mathbf{x}_0$ and $\mathbf{C}_0$.

If the forward operator $\mathbf{h}_t(\mathbf{x})$ is linear, it can be proven that the final estimates of the model parameters $[\hat{\mathbf{x}}, \hat{\mathbf{C}}]$ do not depend on the initial guess $[\hat{\mathbf{x}}_0, \hat{\mathbf{C}}_0]$ (Catlin 1989, Kalman 1960). In the case of a non-linear forward operator, even if not rigorously proven, this independence can be valid for the asymptotic result $[\bar{\mathbf{x}}, \bar{\mathbf{C}}]$ of an iterative application of the KF procedure on the same experimental data. For a finite number N of global iterations of the KF process the resulting estimate of the model parameters can depend on the initial guess since multiple local minima and corresponding attraction basins may exist. The KF procedure, in fact, implicitly minimizes a norm of the difference between the experimental and computed data, which not necessarily is a convex function of the parameter vector $\mathbf{x}$, and therefore local minima may exist. Points within the right attraction basin, and also as close as possible to the absolute minimum should be selected as initial guess in order to speed up the convergence of the method.

4 NUMERICAL APPLICATIONS

The experimental data used for the identification problem presented in the previous Sections are the uniaxial tensile size effect tests on dog-bone shaped specimens performed in the Stevinlab of Delft University of Technology (van Vliet 1998, 2000). The specimen shape and dimensions for the adopted size range are shown in Figure 2.

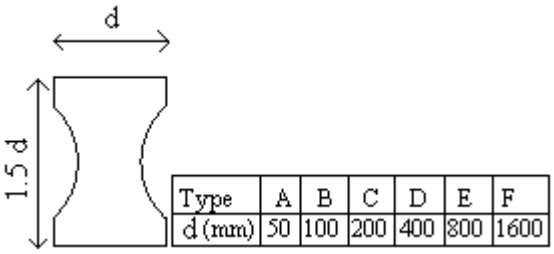

Type	A	B	C	D	E	F
d (mm)	50	100	200	400	800	1600

Figure 2. Specimen shape and dimensions for the adopted size range of the tensile size effect tests.

In order to limit the computing time, only the gradient parameter c and the two softening law parameters α and β are considered in the identification problem. The other model parameters are considered as a priori known and their values, measured in standard tests, are E=33000 [MPa], ν=0.2, κ_i=0.0001, η=14.55.

The experimental data available are the global load-displacement curves of all the specimen sizes. The load is defined as the total force applied at the end of the specimen. The deformation is the average value of all the LVDTs placed in the middle of the specimen with a scaled measurement length (van Vliet 2000).

4.1 *KNN method application*

The experimental quantities collected in the vector $\mathbf{y}_{exp}$ are represented by 100 points along the global load-displacement curve of each specimen size. In other words 100 total forces are considered in correspondence with 100 fixed and equally spaced deformations, so that the Equation 12 may be rewritten as:

$$f(\mathbf{x}) = \sum_{j=1}^{100} \frac{1}{s_{e,j}^2} (\mathrm{F}_{\mathrm{comp,j}}(\mathbf{x}) - \mathrm{F}_{\mathrm{exp},j})^2 \qquad (23)$$

The parameters population selected for the evaluation of $\mathbf{y}_{comp}$ is represented by the sets generated by all the combinations of the values given in Table 1. For each specimen size a total number of 9x7x3=189 forward problems have to be solved in order to compute the $\mathbf{y}_{comp}$ vector corresponding to each parameters set $\mathbf{x}_i$.

Table 1. Values for the generation of the parameter sets population.

Parameter	c [mm^2]	β	α
Value n. 1	20.0	1500.0	0.93
Value n. 2	25.0	1400.0	0.94
Value n. 3	30.0	1300.0	0.95
Value n. 4	35.0	1200.0	-
Value n. 5	40.0	1100.0	-
Value n. 6	45.0	1000.0	-
Value n. 7	50.0	900.0	-
Value n. 8	-	800.0	-
Value n. 9	-	700.0	-

The plot of the approximated surface $f(\mathbf{x})$ as function of c and β, starting from the 189 points $f(\mathbf{x}_i)$, is shown in Figure 3, for all the specimen sizes (except type F, omitted because of the large computational effort). Figure 3 is related to α=0.93, having analogous results for the other values of α. The objective function $f(\mathbf{x})$ has basically a saddle shape and the promising region for the parameters estimation is a diagonal area. Sections of $f(\mathbf{x})$ with planes perpendicular to the β axis may be approximated by the following regression formula:

$$f(c)\Big|_{\substack{\alpha=\overline{\alpha} \\ \beta=\overline{\beta}}} = b_1 c^3 + b_2 c^2 + b_3 c^1 + b_4 \qquad (24)$$

The (cubic) curves represented by Equation 24 are plotted in Figure 4 for all values of β, in case of specimen type B and for α=093.

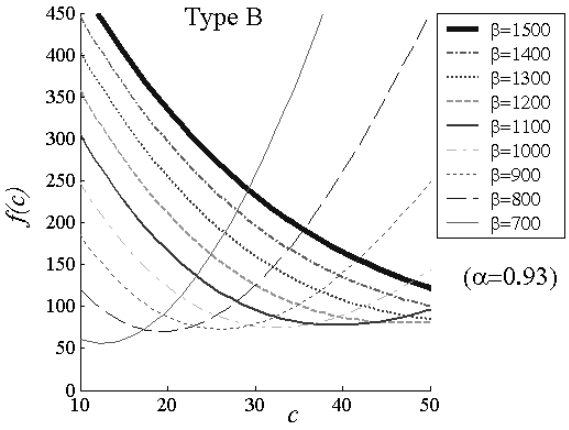

Figure 4. Sections of the objective function $f(\mathbf{x})$ with planes perpendicular to the β axis, for specimen type B and α=0.93.

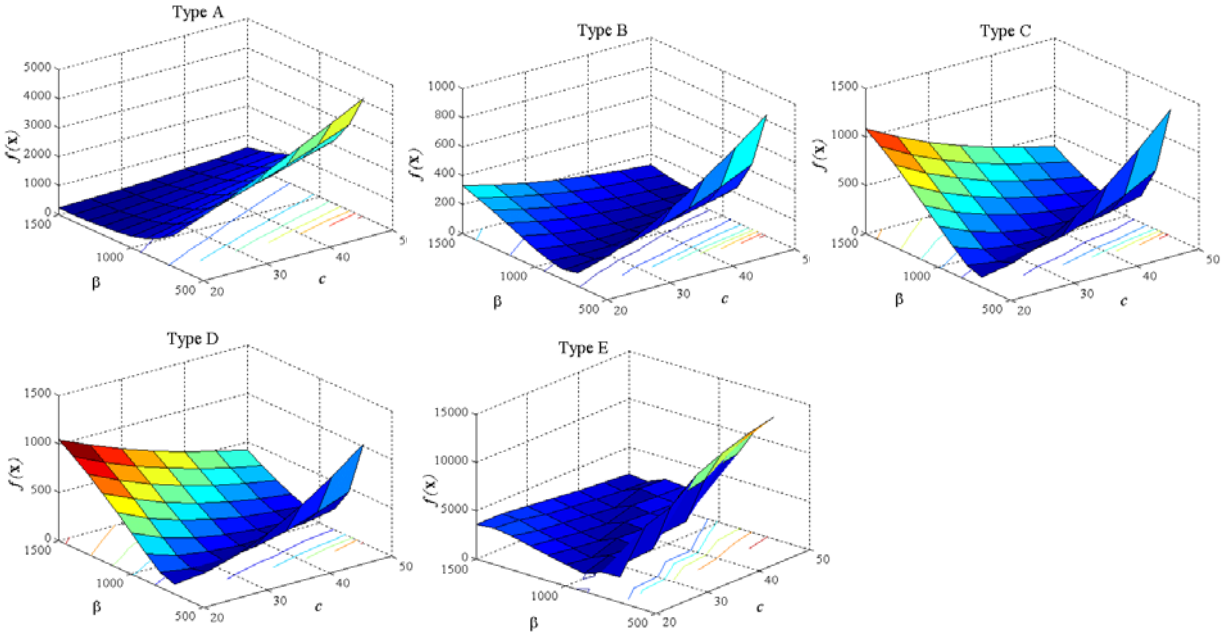

Figure 3. Objective function $f(\mathbf{x})$ for different specimen sizes. In all cases $\alpha = 0.93$.

Moving along the diagonal area that corresponds to the saddle of the objective function, different minima can be found. The gradient parameter c and the softening law parameter β are strictly correlated and the inverse problem is ill posed, since different parameter sets give the same global response of the specimen. However, the displacement field and the damage distribution in the process zone resulting from equivalent parameter sets may be different, so that experimental local information near the crack may be used in order to select the best parameter set (Carmeliet 1999). Another possible way to regularize the problem is the introduction of an initial guess of the model parameters in the objective function $f(\mathbf{x})$, so that, analogously to Equation 18, Equation 11 may be rewritten as:

$$f(\mathbf{x}) = \mathbf{e}^T \mathbf{C}_{\text{exp}}^{-1} \mathbf{e} + (\mathbf{x} - \mathbf{x}_0)^T \mathbf{C}_0^{-1} (\mathbf{x} - \mathbf{x}_0) \qquad (25)$$

The initial guess $\mathbf{x}_0$ and the associated covariance $\mathbf{C}_0$ play a key role and the objective function takes a convex shape, as shown in Figure 5.

However, the identified model parameters may be strongly influenced by the initial guess and small values of $\mathbf{C}_0$ may result in a biased estimation.

Different diagonal promising areas are found for the various specimen sizes, as shown in Figure 6,

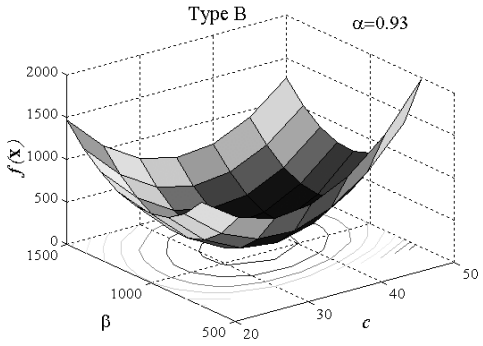

Figure 5. Objective function with initial guess (type B).

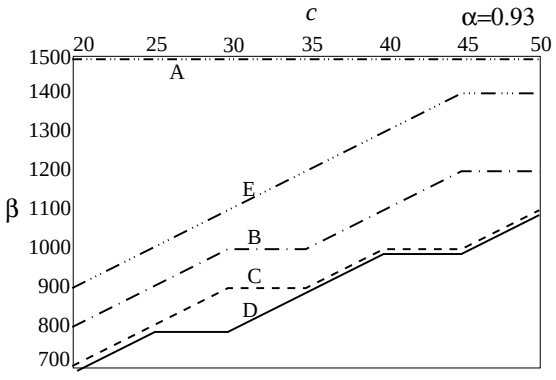

Figure 6. Parameter sets corresponding to the promising areas for the various specimen sizes, for α=0.93.

where the lines corresponding to the best parameter sets are plotted on the parameters grid for all the specimen types (case α=0.93).

The horizontal line corresponding to the specimen type A, in Figure 6, denotes that the chosen parameter grid is not correct for that specimen size. Regions of higher values of β correspond to better parameter estimations in the case of the smallest specimen size.

The best parameter set, corresponding to the nearest neighbor $\mathbf{y}_{comp}$ of $\mathbf{y}_{exp}$, for each specimen size is presented in Figure 7("o" marker).

However, if the peak load is considered in Equation 23 (i.e. j=1) to find the parameter set that, among the considered population, gives the best reproduction of the maximum load carried by the specimen, different parameter estimations are obtained (see Fig 7, "+" marker).

Using these estimations, the size effect curve can be computed. Although different parameter sets are considered for each specimen size ("+" marker in Fig. 7), the calculated size effect curve is too flat, as shown in Figure 8 (Lehký & Novák 2002). The absolute minimum of the optimization problem can not be found in the considered parameter grid for the specimen type A and E.

4.2 *KF method*

Four KF procedures are considered in order to investigate the influence of $\mathbf{C}_0$, $\mathbf{C}_{exp}$ and number of KF steps on the estimated parameter values, for the specimen type B. The related data are reported in Table 2, expressing the covariance matrixes in terms of uncertainty on the mean values.

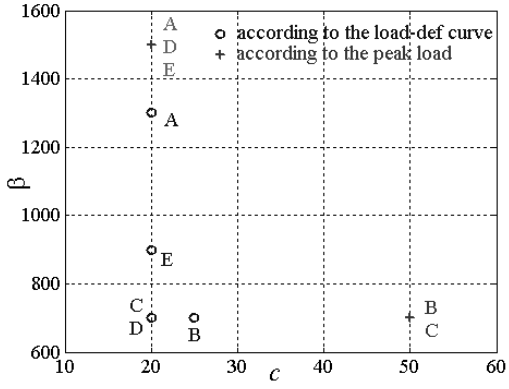

Figure 7. Best parameter sets for all specimen types, corresponding to the best global load-displacement curve and to the best the peak load.

Table 2. KF procedures data

KF procedure	C_0 [%]	C_{exp} [%]	n. steps
KF_I (ref.)	40	50 (real)	20
KF_{II}	10	50	20
KF_{III}	40	5	20
KF_{IV}	40	50	30

In order to limit the computing time (forward finite difference scheme is used for the numerical evaluation of the sensitivity matrix), only two parameters are involved in the identification procedure, considering α as a priori known (α=0.95).

The initial guess for all the KF procedures is taken equal to $\mathbf{x}_0^T=[\beta_0\ c_0]=[1200\ \ 40]$.

The estimated parameter values of the four KF procedures are represented in Figure 9 on the same parameter grid used earlier for the KNN method. Also the minima of the surface $f(\mathbf{x})$ (see Fig. 6, type B) are reported in the same figure.

A decrease in $\mathbf{C}_0$ corresponds to a decrease in the uncertainty of the initial guess and, as a consequence, the final parameter estimate is forced to be close to the initial point, as observed for the case of KF_{II}. The best result, among the four procedures, is obtained by the KF_{III}. A small uncertainty of the experimental information forces the procedure to obtain computational results as close as possible to the experimental data. The final estimation is improved by increasing the number of KF steps, as in the case of KF_{IV}.

The parameter sets identified by the considered KF procedures converge to the same local minimum (except KF_{II}), being the starting point in that attraction basin.

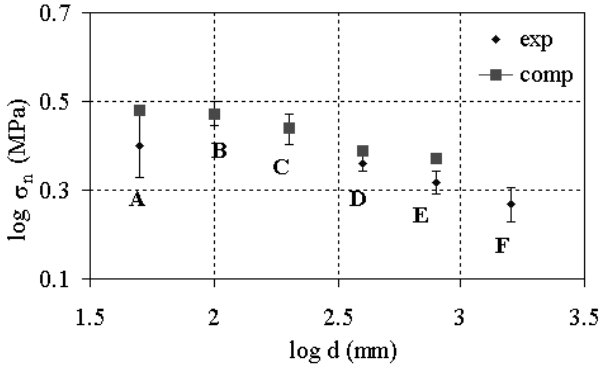

Figure 8. Experimental and computational nominal strength σ_n vs. specimen size d.

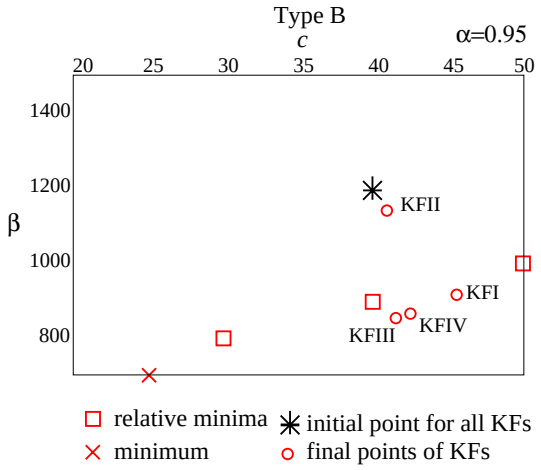

Figure 9. Estimated parameter sets for KF_I, KF_{II}, KF_{III}, KF_{IV}.

5 CONCLUSIONS

The parameter identification based only on global information of a single tensile test may result in an ill posed problem with a non-unique solution. The objective function of the minimization problem may be regularized by adding local information on the process zone or an initial guess on the model parameters. The estimate of $\mathbf{x}_0$ and the associated covariance $\mathbf{C}_0$ is a crucial point, since the identified parameters may be strongly influenced by this choice.

Diagonal promising areas in the parameter space of c and β characterize the examined inverse problem, so that the gradient parameter is correlated with the softening law parameter β in terms of global response of the specimen.

The parameter identification based only on the peak loads of size effect tests may give different results than identification based on the entire global force-deformation response of the specimens. However the gradient damage model, with only one parameters set, can not reproduce the experimental size effect curve of the considered dog-bone specimens.

The Kalman filter technique is a powerful tool that identifies not only the model parameters, but also the related uncertainty. However the non linearity of the problem does not guarantee the independence of the final parameters estimate from the initial guess, which is a weak point for many numerical applications.

6 ACKNOWLEDGEMENTS

The program related to the implementation of the gradient-enhanced model in the framework of the finite element code FEAP was kindly supplied by A. Simone.

The authors also like to acknowledge M. R .A. van Vliet for having supplied the experimental results and the Technical Science Foundation in the Netherlands (STW) for the financial support.

REFERENCES

Bažant, Z.P. & Pijaudier-Cabot, G. 1988. Nonlocal continuum damage, localization, instability and convergence. *Journal of Applied Mechanics* 55: 287-293.

Beck, J.V. & Arnold, K.V. 1977. *Parameter Estimation in Engineering and Science*. New York: Wiley.

Bittanti, S., Maier, G. & Nappi, A. 1984. Inverse problem in structural elastoplasticity: a Kalman filter approach. In A. Sawczuk & G. Bianchi (eds.), *Plasticity Today:* 311-329. London: Elsevier Applied Science Publ.

Bolzon, G., Fedeli, R. & Maier, G. 2002. Parameter identification of a cohesive crack model by Kalman filter. *Computer methods in Applied Mechanics in Engineering*, 191: 2847-2871.

Bui, H.D. 1994. *Inverse Problem in the Mechanics of Materials: an Introduction*. London: CRC Press.

Carmeliet, J. 1999. Optimal estimation of gradient damage parameters from localization phenomena in quasi-brittle materials. *Mechanics of Cohesive-Frictional Materials*, 4: 1-16.

Catlin, D.E. 1989. *Estimation, Control and the Discrete Kalman Filter*. Berlin: Springer Verlag, Applied Mathematical Sciences.

Iacono, C., L.J. Sluys & van Mier, J.G.M. 2003. Development of an inverse procedure for parameter estimates of numerical models. In N. Bićanić, R. de Borst, H. Mang & G. Meschke (eds.), *Computational Modelling of Concrete Structures; Proc. Euro_c Conf., St. Johann im Pongau, Austria, 17-20 March 2003*. Rotterdam: Balkema.

Kailath, T., Sayed, A.H. & Hassibi, B. 2000. *Linear Estimation*. London: Prentice Hall.

Lehký, D. & Novák, D. 2002. Modeling of size effect in concrete under uniaxial tension. *4th International Ph. D. Symposium in Civil Engineering.* Munich, Germany, vol. 1, ISBN 3-935065-09-4, 2002, pp. 435-444.

Peerlings, R.H.J., de Borst, R., Brekelmans W.A.M. & de Vree J.H.P. 1996. Gradient-enhanced damage for quasi-brittle materials. *International Journals for Numerical Methods in Engineering* 39: 3391-3403.

Peerlings, R.H.J. 1999. *Enhanced Damage Modelling for Fracture and Fatigue.* Ph. D. thesis, Eindhoven University of Technology, The Netherlands.

Tarantola, A. 1987. *Inverse Problem Theory. Methods for Data Fitting and Model Parameter estimation*. Southampton: Elsevier Applied Science.

Van Vliet, M.R.A. & van Mier, J.G.M. 1998. Experimental investigation of size effect in concrete under uniaxial tension. *Int. Conf. FraMCos-3, Gifu, Japan, October 1998*. Freiburg, Germany: Aedificatio Publishers.

Van Vliet, M.R.A. 2000. *Size Effect in Tensile Fracture of Concrete and Rock.* Ph. D. thesis, Delft University of Technology, The Netherlands.